

## ESI

### **A low-dimensional molecular spin system with two steps of magnetic transitions and liquid crystal property**

Hai-Bao Duan<sup>†</sup> Xiao-Ming Ren<sup>†#\*</sup> Lin-Jiang Shen<sup>†</sup> Wan-Qin Jin<sup>†</sup> Qing-Jin Meng<sup>#</sup>  
Zheng-Fang Tian<sup>†</sup> Shi-Ming Zhou<sup>ξ\*</sup>

<sup>†</sup> State Key Laboratory of Materials-Oriented Chemical Engineering and College of Science, Nanjing University of Technology, Nanjing 210009, P.R. China

<sup>#</sup> State Key Laboratory & Coordination Chemistry Institute, Nanjing University, Nanjing 210093, P. R. China

<sup>ξ</sup> Hefei National Laboratory for Physical Sciences at Microscale, University of Science and Technology of China, Hefei, Anhui 230026, P. R. China

Tel.: +86-25-83587820

Fax: +86-25-83587438

E-mail: [xmren@njut.edu.cn](mailto:xmren@njut.edu.cn); [zhousm@ustc.edu.cn](mailto:zhousm@ustc.edu.cn)

**Table S1:** Crystallographic and refinement Data for the tapped phase at 293 K

Molecular formula	$C_{13}H_{19}N_6NiS_4$
Molecular mass	446.30
crystal system	monoclinic
Space group	P2(1)/m
a/Å	4.4980(3)
b/Å	20.5770(14)
c/Å	13.6962(9)
$\alpha^\circ$	90
$\beta^\circ$	96.193(6)
$\gamma^\circ$	90
V/Å <sup>3</sup> / Z	1260.24(15) / 2
$\mu/\text{mm}^{-1}$	4.263
F(000)	462
$\rho/\text{g cm}^{-3}$	1.176
R <sub>1</sub>	0.1989
wR <sub>2</sub>	0.5476
Goodness of fit on F <sup>2</sup>	2.427

**Table S2:** Crystallographic and refinement Data for **1** at 293 K and 105 K

Complex	<b>1</b> at 293 K	<b>1</b> at 105 K
Molecular formula	$C_{19}H_{19}N_6NiS_4$	$C_{19}H_{19}N_6NiS_4$
Molecular mass	518.37	518.37
crystal system	Triclinic	Triclinic
Space group	P -1	P -1
a/Å	4.5025(6)	4.4540(5)
b/Å	13.6474(13)	13.6238(15)
c/Å	20.5060(19)	20.238(2)
$\alpha^\circ$	84.901(8)	84.472(9)
$\beta^\circ$	85.132(9)	85.962(8)
$\gamma^\circ$	83.759(9)	82.683(9)
V/Å <sup>3</sup> / Z	1244.0(2) / 2	1210.3(2) / 2
$\mu/\text{mm}^{-1}$	4.405	4.528
F(000)	534.0	532.0
$\rho/\text{g cm}^{-3}$	1.384	1.422
R <sub>1</sub>	0.0472	0.0441
wR <sub>2</sub>	0.1678	0.1397
Goodness of fit on F <sup>2</sup>	1.127	1.227

**Table S3:** Selected Bond Lengths (Å) and Bond Angles (°) for **1** at 293 K and 105 K

<b>1</b> at 293 K			
Ni(1)-S(1)	2.134(1)	Ni(2)-S(3)	2.136(1)
Ni(1)-S(2)	2.147(1)	Ni(2)-S(4)	2.151(1)
S(1)-Ni(1)-S(1A)	180.00(1)	S(3)-Ni(2)-S(3A)	180.00(6)
S(1)-Ni(1)-S(2)	87.58(5)	S(3)-Ni(1)-S(4A)	92.56(5)
S(1A)-Ni(1)-S(2)	92.42(5)	S(3)-Ni(1)-S(4)	87.44(5)
<b>1</b> at 105 K			
Ni(1)-S(1)	2.138(1)	Ni(2)-S(3)	2.143(1)
Ni(1)-S(2)	2.152(1)	Ni(2)-S(4)	2.155(1)
S(1)-Ni(1)-S(1A)*	180.00(6)	S(3)-Ni(2)-S(3A)	180.00(5)
S(1)-Ni(1)-S(2)	87.23(5)	S(3)-Ni(1)-S(4A)	92.69(5)
S(1A)-Ni(1)-S(2)	92.77(5)	S(3)-Ni(1)-S(4)	87.31(5)

Symmetric code: A = 1-x, 1-y, 1-z

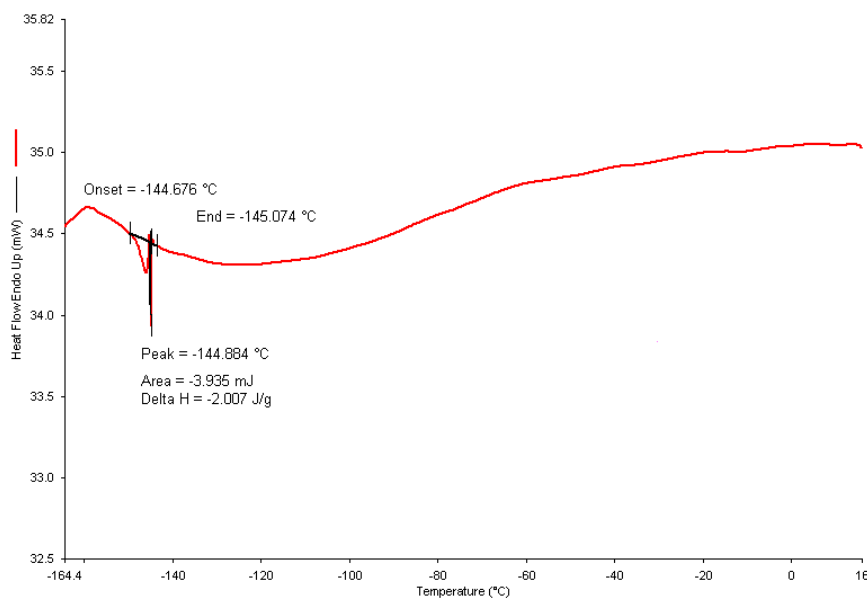


Figure S1 DSC plot of as-prepared sample of **1** measured from -164 to 16 °C shows an enthalpy change corresponding to the magnetic transition in low-temperature region ( $T_C \approx 128.5$  K).

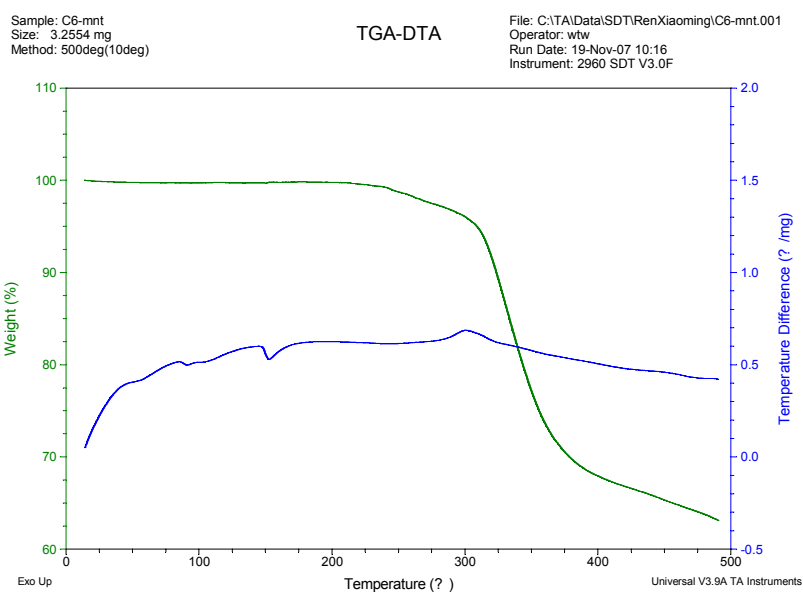


Figure S2 TGA and DTA curves for as-prepared sample of **1** (the measurements were performed under  $N_2$  atmosphere) in 20-500 °C range disclosed that **1** is thermally stable below 237 °C; the weight losing is about 5% in 237-307 °C and 32% in 307-500 °C ranges.

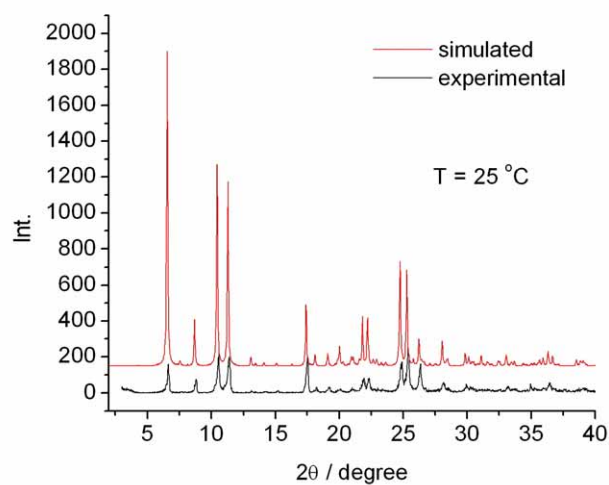


Figure S3 Powder X-ray diffraction patterns at 25 °C (experimental and simulated profiles) for as-prepared sample of **1** which confirms the phase purity of the as-prepared sample.

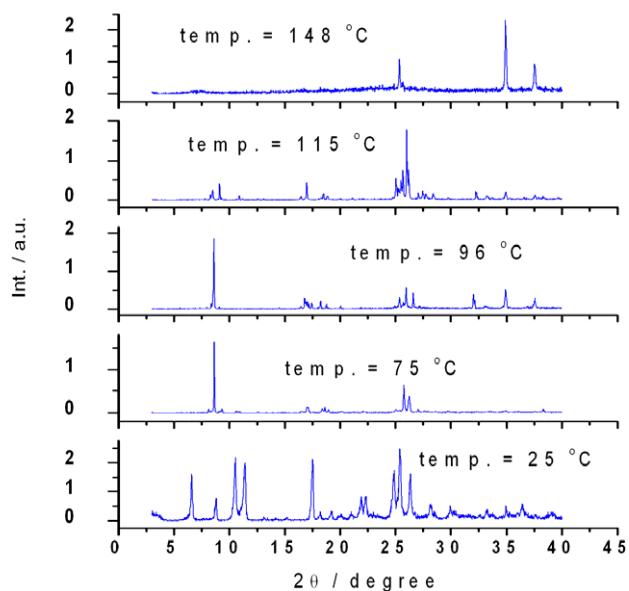


Figure S4 PXRD patterns were measured from 25 (crystal) to 148 °C (mesophase) in the  $2\theta$  range of 3-40° for **1**.

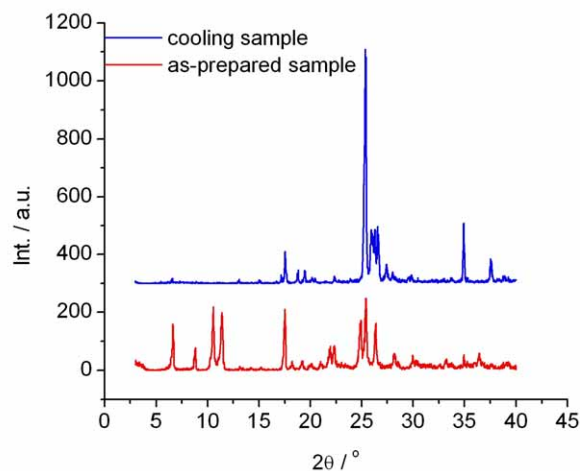


Figure S5 PXR D profiles measured for the as-prepared sample and the cooling sample after melted at  $25^\circ\text{C}$  in the  $2\theta$  range of  $3\text{--}40^\circ$  for **1**, which show different patterns.

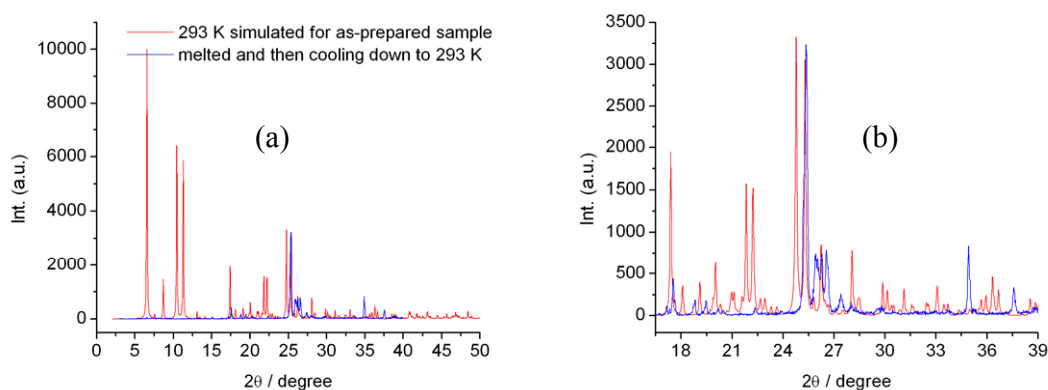


Figure S6 PXR D profiles (Figure b is an enlarged one of Figure a), in which the red line represents the simulated PXR D pattern for the as-prepared sample of **1** from the single crystal data at 293 K and the blue line is the experimental PXR D pattern for the sample that is melted and then cooling down to  $25^\circ\text{C}$  for **1**. From Figure b, the somewhat difference are observed between two patterns although they are similar to each other.

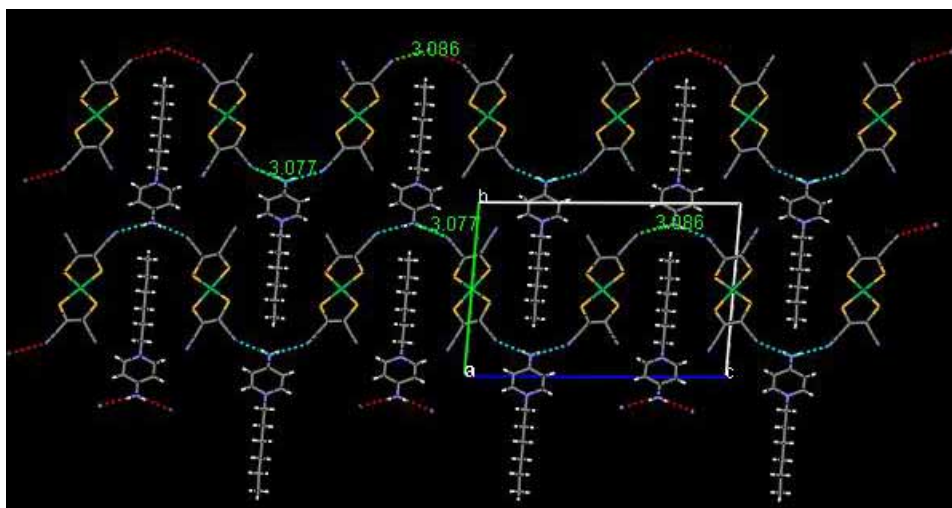
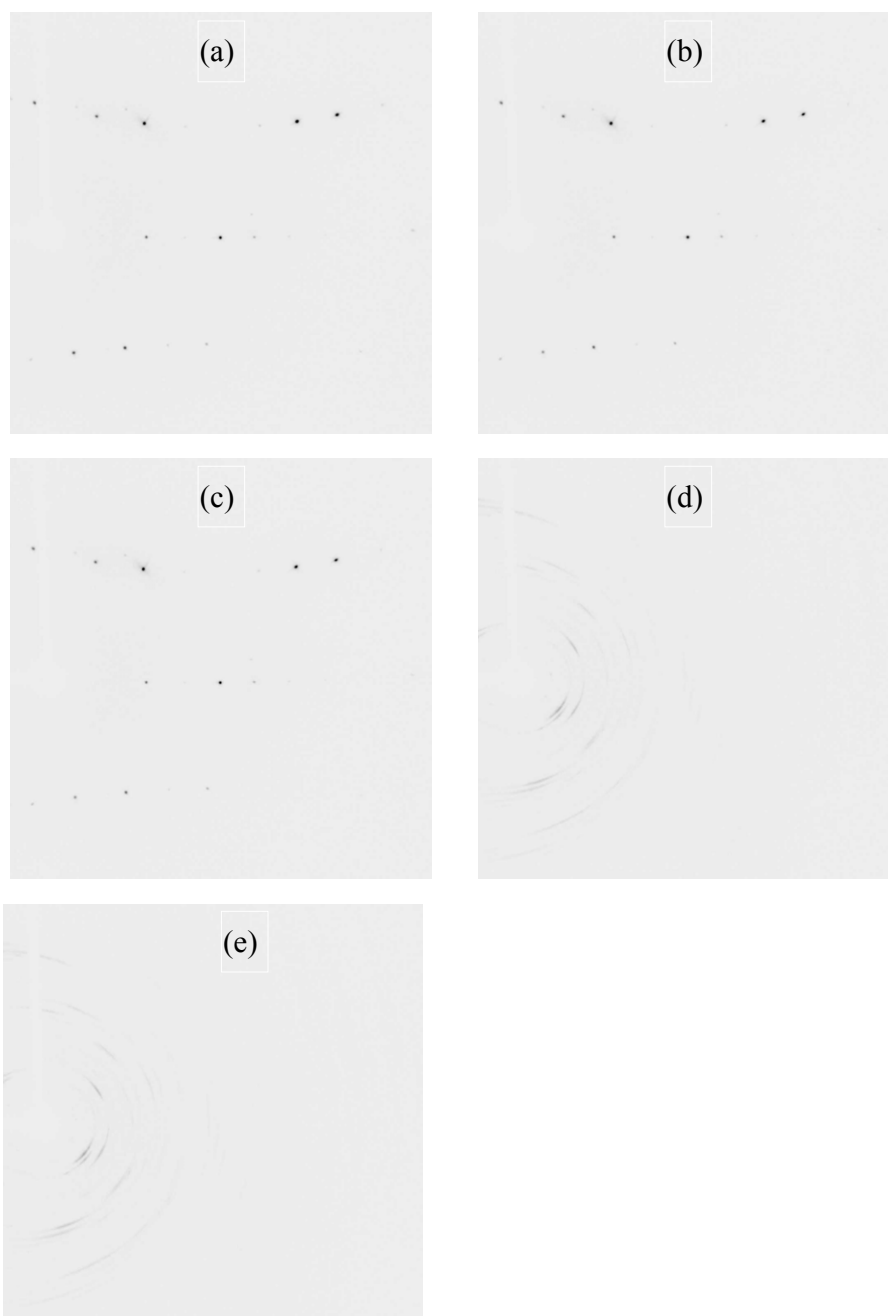


Figure S7 H-bonding sheet which is parallel to bc-plane (projected along a-axis) at 25 °C for as-prepared sample.



**Figure S8** Diffractions change with temperature measured at (a) 320 K (b) 330 K (c) 345 K (d) 355 K and (e) 320 K after cooling.

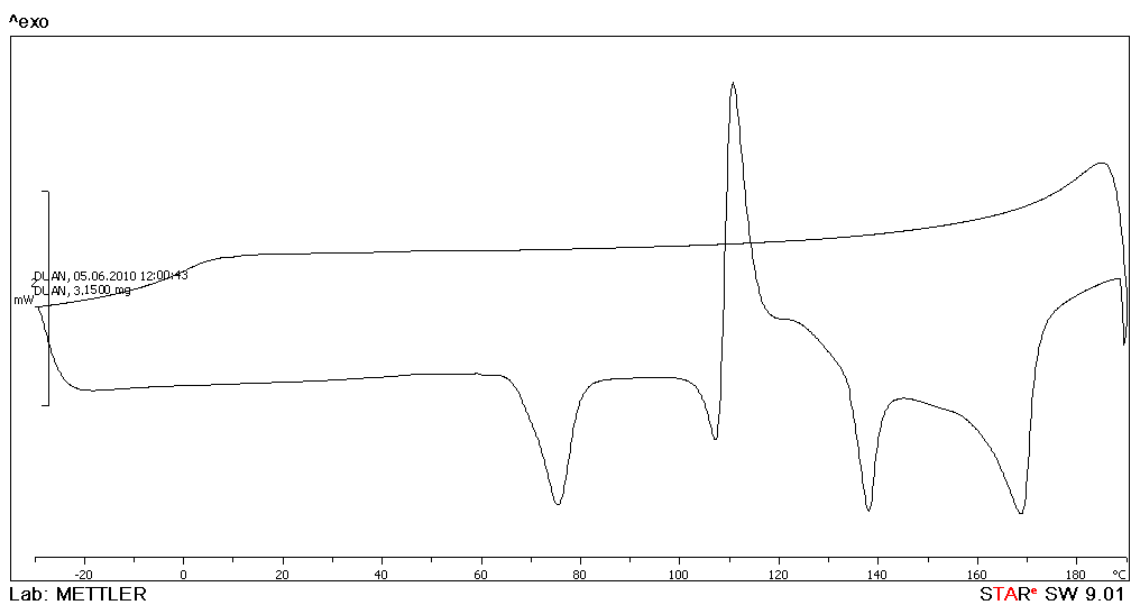
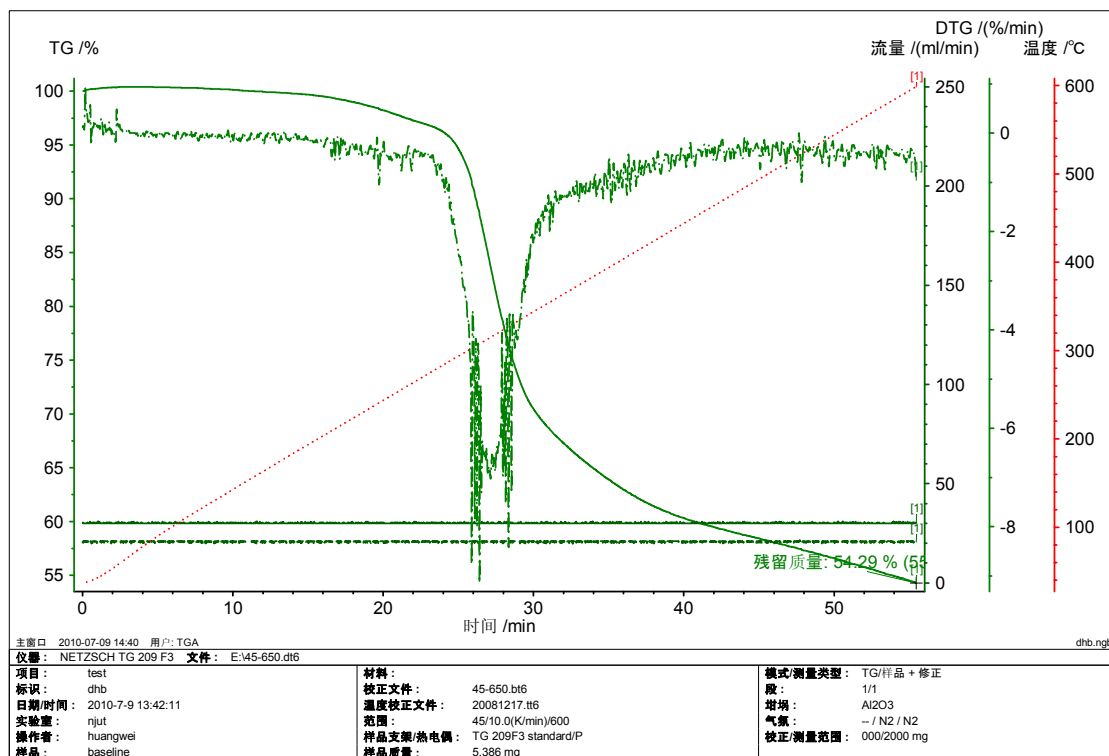
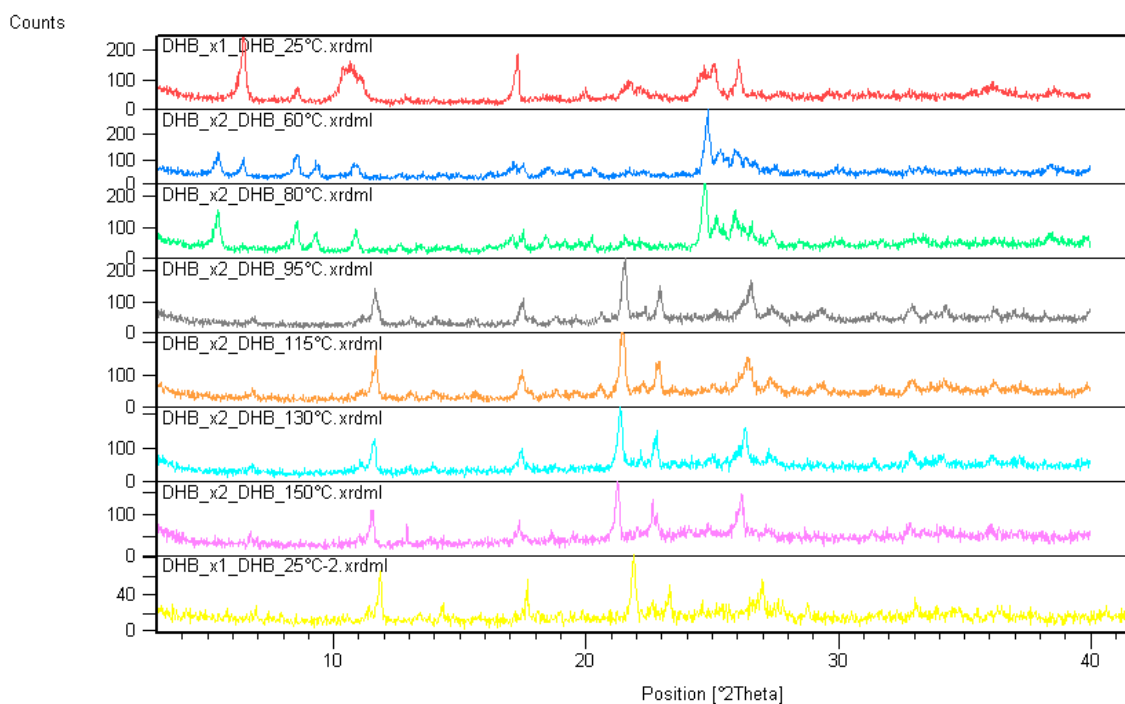
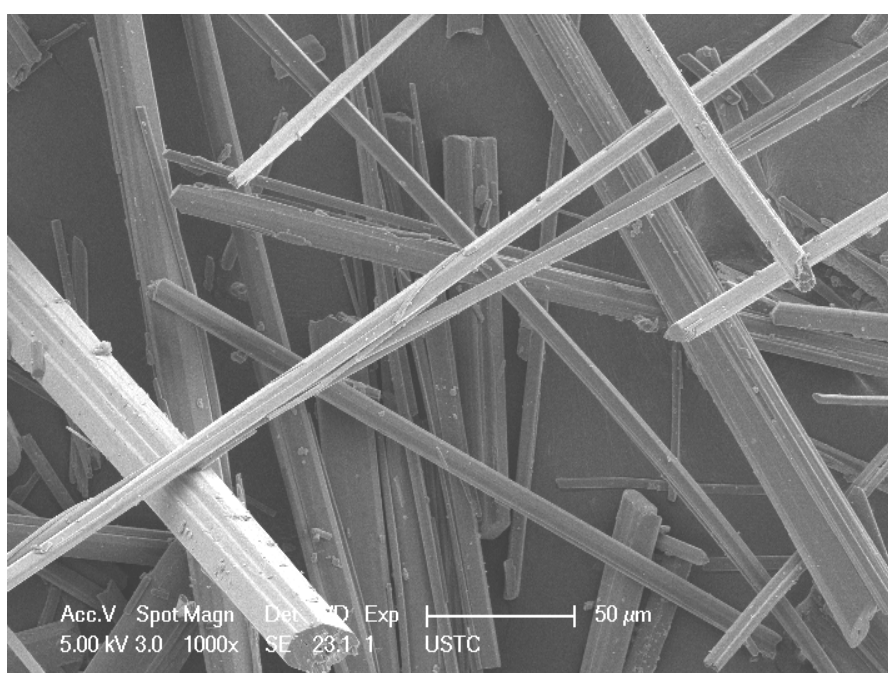
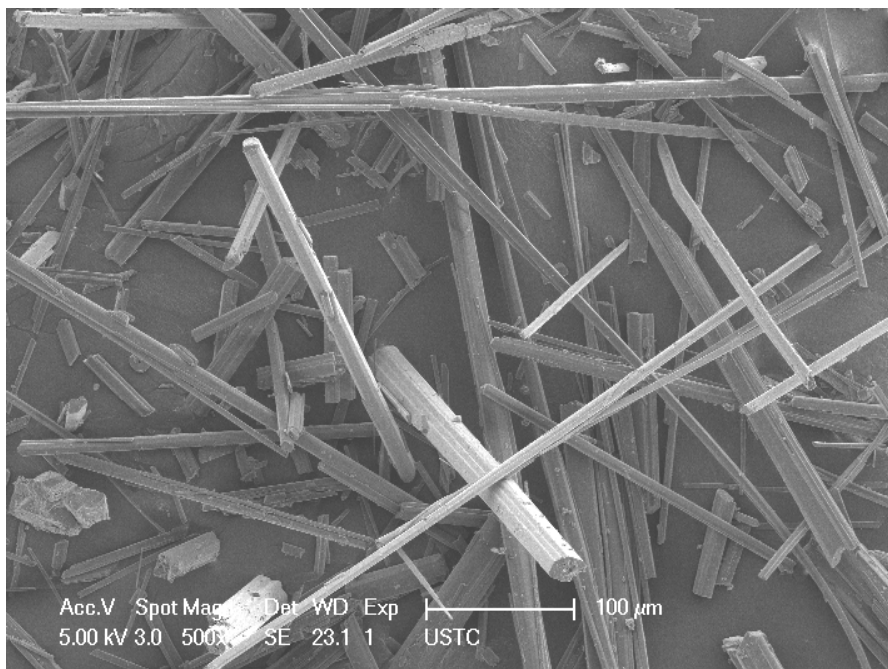


Figure S9 TG and DSC profile of  $[C_6-APy][Cu(mnt)_2]$ .



**Figure S10** Temperature dependent PXRD for  $[C_6-APy][Cu(mnt)_2]$  (the measurements in sequence of 25 °C→60→80→95→115→130→150→25 °C).



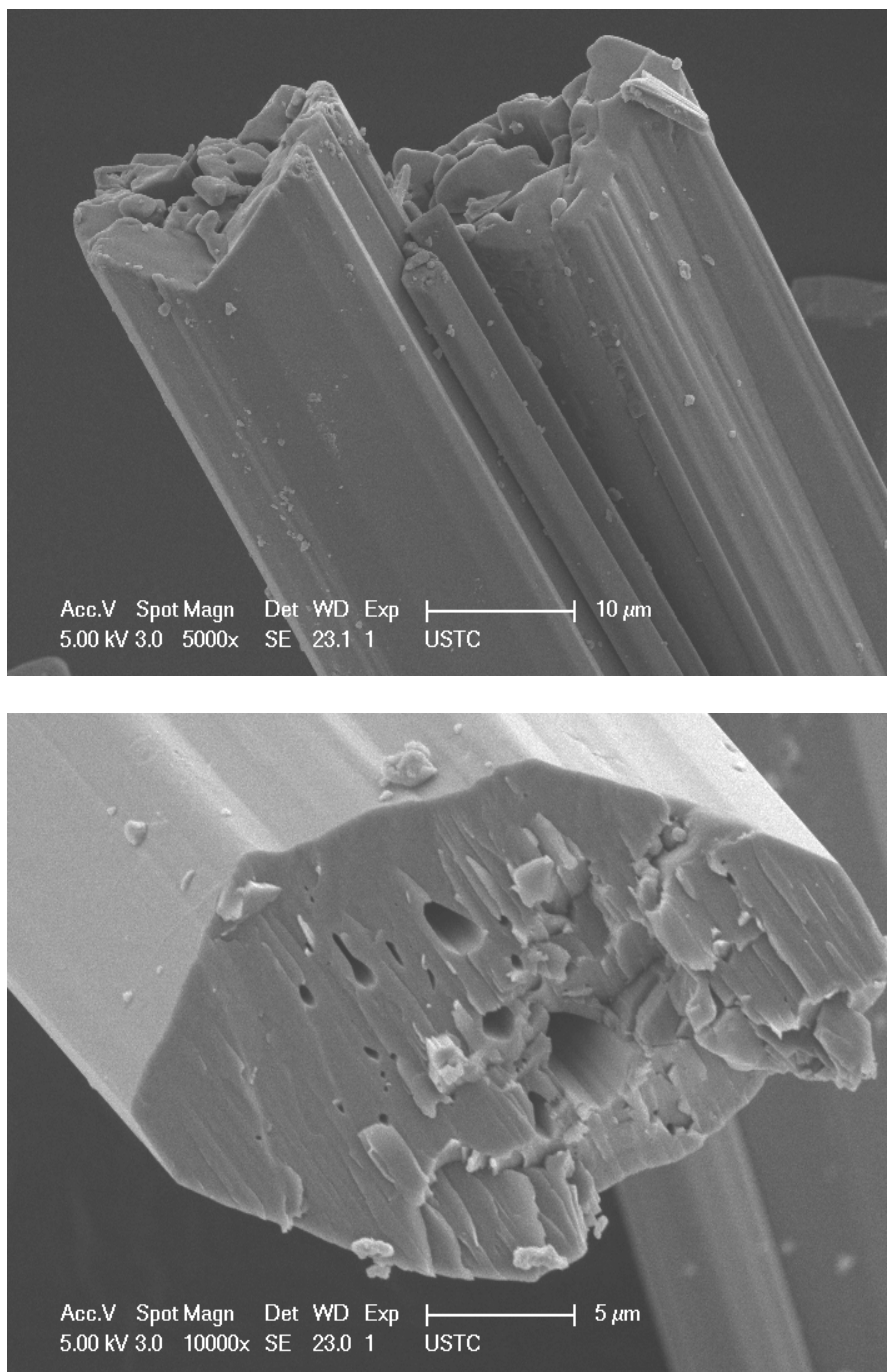


Figure S11 SEM micrographs of  $[C_6-APy][Cu(mnt)_2]$ .